Acta Pharmacologica Sinica (2018) 39: 1305–1316
 1671-4083/18
www.nature.com/aps

Article

Biological characterization of human amniotic epithelial cells in a serum-free system and their safety evaluation

Peng-jie YANG[1, 2, 3], Wei-xin YUAN[1, 2, 3], Jia LIU[4], Jin-ying LI[1, 2, 3], Bing TAN[1, 2, 3], Chen QIU[1, 2, 3], Xiao-long ZHU[1, 2, 3], Cong QIU[1, 2, 3], Dong-mei LAI[5], Li-he GUO[6, 7], Lu-yang YU[1, 2, 3, *]

[1]Institute of Genetics and Regenerative Biology, College of Life Sciences, [2]College of Life Sciences-iCell Biotechnology Regenerative Biomedicine Laboratory, [3]Center for Stem Cell and Regenerative Medicine, Zhejiang University, Hangzhou 310058, China; [4]Life Science College, Zhejiang Chinese Medical University, Hangzhou 310053, China; [5]International Peace Maternity and Child Health Hospital, School of Medicine, Shanghai Jiao Tong University, Shanghai 200030, China; [6]Institute of Biochemistry and Cell Biology, Shanghai Institutes for Biological Sciences, Chinese Academy of Sciences, Shanghai 200031, China; [7]Shanghai iCELL Biotechnology Co Ltd, Shanghai 200333, China

Abstract

Human amniotic epithelial cells (hAECs), derived from the innermost layer of the term placenta closest to the fetus, have been shown to be potential seed cells for allogeneic cell therapy. Previous studies have shown a certain therapeutic effect of hAECs. However, no appropriate isolation and culture system for hAECs has been developed for clinical applications. In the present study, we established a serum-free protocol for hAEC isolation and cultivation, in which better cell growth was observed compared with that in a traditional culture system with serum. In addition to specific expression of cell surface markers (CD29, CD166 and CD90), characterization of the biological features of hAECs revealed expression of the pluripotent markers SSEA4, OCT4 and NANOG, which was greater than that in human mesenchymal stem cells, whereas very low levels of HLA-DR and HLA-DQ were detected, suggesting the weak immunogenicity of hAECs. Intriguingly, CD90+ hAECs were identified as a unique population with a powerful immunoregulatory capacity. In a systemic safety evaluation, intravenous administration of hAEC did not result in hemolytic, allergy, toxicity issues or, more importantly, tumorigenicity. Finally, the therapeutic effect of hAECs was demonstrated in mice with radiation-induced damage. The results revealed a novel function of hAECs in systemic injury recovery. Therefore, the current study provides an applicable and safe strategy for hAEC cell therapy administration in the clinical setting.

Keywords: human amniotic epithelial cells; cell therapy; safety evaluation; serum-free

Acta Pharmacologica Sinica (2018) 39: 1305–1316; doi: 10.1038/aps.2018.22; published online 22 Mar 2018

Introduction

With the potential for replication and multidirectional differentiation, stem cells are some of the best candidates for cellular therapy and regenerative medicine. However, the transition from bench-side to bedside is challenged by tumorigenicity, immune responses, multi-step procedures and ethical concerns according to studies of embryonic stem cells (ESCs) and induced pluripotent stem cells (iPSs)[1-3]. Although cell therapy using autologous stem cells circumvents some of these issues, maintaining quality control and industrial production is difficult due to individual differences in cell sources[4].

Recently, researchers have started to focus on the stem-like cells in the amniotic membrane (AM). The AM is the innermost layer of the placenta and is important for maternal-fetal material exchange. Human amnion epithelial cells (hAECs), isolated from the layer closest to the fetus in the term placenta, are considered a unique and ideal cell source for cell therapy[5]. Our previous study and other reports indicated that hAECs were pluripotent and could differentiate into three germ layers *in vitro* and *in vivo*[6-8], which could be attributed to their derivation from the inner cell mass within the blastocyst at d 8 of fertilized egg development. OCT4, the key transcription factor for maintaining pluripotency and self-renewal in ESCs and iPSs, is expressed in hAECs[2, 7, 9]. Most of the other representative pluripotent stem cell markers, such as NANOG, SOX-2, SSEA-4, FGF-4, and REX-1, have also been detected in

*To whom correspondence should be addressed.
E-mail luyangyu@zju.edu.cn
Received 2017-11-25 Accepted 2018-01-01

hAECs[7]. However, hAECs lack telomerase, resulting in a limited proliferative capacity[7]. On the other hand, particularly low expression of HLA class I molecules has been reported in hAECs[10, 11], suggesting potential immune tolerance after transplantation. Furthermore, immuneregulatory properties of hAECs have been demonstrated *in vitro* and in animal models[12-14], corresponding to the function of the AE in maintaining feto–maternal tolerance during pregnancy.

All of these qualities suggest that hAECs represent an excellent candidate for allogeneic cell therapy in the clinic. Indeed, several studies have revealed the therapeutic effects of hAECs for injury repair in ophthalmology[15-19], wound healing[20, 21] and pulmonary and liver fibrosis[22]. However, an appropriate isolation and culture system for hAECs aimed at clinical applications is not currently available. In the present study, we established a serum-free protocol for hAEC isolation and cultivation. A systemic biological characterization and safety evaluation demonstrated the applicable properties and safety of cell therapy. In addition, the therapeutic capability of hAECs was identified in mice with radiation-induced injury.

Materials and methods

hAEC isolation and culture

Human amnion membranes were obtained with written and informed consent from healthy mothers undergoing cesarean section. Human placentas were obtained from healthy mothers who provided written informed consent after uncomplicated elective cesarean section. The procedure was approved by the institutional patients and ethics committee of the International Peace Maternity and Child Health Hospital, Shanghai Jiaotong University School of Medicine. All donors were negative for hepatitis A, B, C, and D and HIV-I and TPAB (Treponema pallidum antibody). hAECs were isolated from the collected placentas. In brief, the amniotic membrane was peeled from the placental chorion and washed in HBSS (Hank's balanced salt solution) to remove blood cells. The amniotic membrane was digested with 0.25% trypsin (EDTA) for 30 min at 37 °C in a water bath. Two volumes of complete culture medium (F12/DMEM, 10% KSR (KnockOut Serum Replacement), 2 mmol/L *L*-glutamine, 1% nonessential amino acid, 55 μmol/L 2-mercaptoethanol, 1 mmol/L sodium pyruvate, 1% antibiotic-antimycotic (all from Gibco) and 10 ng/mL EGF (Peprotech) were added to the trypsin digestion medium, and the sample was centrifuged for 10 min at 300×*g*. The cell pellet was then suspended in the complete culture medium for the subsequent cell culture. The cultured P1-hAECs were then frozen in CELLBANKER (ZENOAQ, Fukushima, Japan) at a concentration of 5×10^6/mL and stored in a refrigerator at -80 °C overnight. Then, frozen vials were transferred into liquid nitrogen for long-term preservation. hAECs were thawed by gently agitating the vial in a 37 °C water bath after 30 d of storage. Post-thaw cell viability was assessed by Trypan blue exclusion staining and compared with P1 human umbilical cord mesenchymal stem cells that were also frozen in CELLBANKER using the same method. For comparative study, some hAECs were isolated and cultured using traditional culture medium with 10% FBS (Gibco) instead of KnockOut Serum Replacement. Passages 1-3 of hAECs isolated from more than 3 different donors were utilized in this paper.

Flow cytometry

Cells were digested and then washed with PBS. The hAECs were stained using standard protocols with fluorescence-conjugated antibodies targeting CD34, CD45, CD31, CD29, CD166, CD90, HLA-DR, and HLA-DQ (1:20, all from BioLegend). For SSEA4 and TRA-1-60, hAECs were stained with the SSEA4 (1:20, Millipore) and TRA-1-60 (1:20, Millipore) primary antibodies and then incubated with fluorescence-conjugated secondary antibodies. Measurements of cell cycle distribution were obtained using propidium iodide (PI) staining. Flow cytometric analysis was performed with a FACS Calibur instrument (Becton Dickinson, Franklin Lakes, NJ, USA). Isotype controls were used in each experiment.

Immunofluorescence

Cells were washed with PBS and fixed with 4% PFA (in PBS) for 30 min on ice. The cells were then incubated in 0.2% Triton X-100 (in PBS) for 30 min and blocked in 3% horse serum for 1 h at room temperature. Primary antibodies against Cytokeratin (1:200, Abcam), E-cadherin (1:200, Abcam), OCT4 (1:50, Santa Cruz), SSEA4 (1:100, Millipore), and NANOG (1:40, R&D Systems) were incubated with cells for 12 h at 4 °C, followed by incubation with secondary antibodies for another 1 h at room temperature. Nuclei were stained with DAPI.

Cytokine assay

The culture medium was collected after hAECs and PBMCs were cultured alone or after hAECs were co-cultured with PBMC for 3 d. PHA (5 ug/mL, Sigma) was added into the medium to activate the PBMCs. Cytokines in the medium were detected with ELISA kits, including TNFα (Biolegend), IL17, IL10 and IL2 (all from eBioscience), according to the manufacturer's instructions.

Mice

All animal studies were approved by the Institutional Animal Care and Use Committee of Zhejiang University and adhered to the Guide for the Care and Use of Laboratory Animals. NOD/SCID (Non-Obese Diabetic/Severe Combined Immunodeficiency) mice and ICR (Institute of Cancer Research) mice were purchased from Model Animal Research Center of Nanjing University (Nanjing, China), and all the other animals were purchased from Slac Laboratory Animal (Shanghai, China). The animals were acclimated to the room for one week after arrival and were maintained on a normal 12-h light-dark cycle. The animals were housed in conventional cages with free access to a standard pellet diet and water in specific pathogen-free conditions with a temperature of 24±2 °C and 60%–70% relative humidity. Standard wood chips for mice were used as bedding material.

Toxicity test

Eight-week-old male/female ICR mice were used to determine

the most tolerance dose (MTD), and the no observed adverse effect level (NOAEL) was based on clinical observations, general tissue dissection and survival records. Furthermore, acute toxicity tests of hAECs were performed in ICR mice via single iv injection of hAECs (low dose 2.5×10^7 cells/kg, medium dose 5×10^7 cells/kg or high dose 1×10^8 cells/kg) according to the mouse equivalent dose and the MTD. Clinical observations of the toxicity response, including mouse behavior, mental state, mortality and body weight, and gross dissection were evaluated within 14 d. To evaluate the long-term toxicity of hAECs *in vivo*, 6- to 8-week-old SD rats were subjected to iv injection of hAECs (low dose 2.5×10^7 cells/kg or high dose 5×10^7 cells/kg) every two weeks 3 times. Routine blood parameters, blood biochemistry, the coagulation index, hAEC organ distribution, mouse body weight and viscera weight, general tissue histology, cytokine levels, and T cell populations were examined 6 weeks after transplantation.

Hemolysis test

hAECs were diluted using 0.9% NaCl in an ascending gradient from 1:24 to 1:4 (*v*:*v*) to achieve hAEC numbers from 10^6 to 5×10^6. Diluted hAECs were then co-incubated with 2% rabbit red blood cell suspension in 0.9% NaCl at 37 °C for 3 h. Red blood cells incubated with ddH_2O or 0.9% NaCl were used as positive and negative controls, respectively. The hemolysis and coagulation of red blood cells in each sample were observed and recorded every 15 min for 3 h.

Allergy test

Briefly, 2- to 3-month-old Hartley guinea pigs, purchased from Vital River Laboratory Animal Technology (Beijing, China), were randomly divided into 4 groups (6 animals per group) that were given 0.5 mL of saline, 5 mg of BSA, 1.0×10^6 hAECs or 2.0×10^6 hAECs three times per animal by intraperitoneal injection. Fourteen days after the last sensitization, 3 animals in each group were subjected to the first-batch allergy challenge. If the result was negative, then the remaining animals were subjected to the second-batch allergy challenge 21 d after the last sensitization. Allergic reactions were assessed according to the following symptoms: dysphoria, piloerection, trembling, nose scratching, sneezing, cough, polypnea, urination, defecation, lacrimation, dyspnea, wheezing, purpura, gait instability, jumping, gasping, spasms, spinning, Cheyne-Stokes breathing and death.

Tumorigenicity assay

To investigate the tumorigenicity of hAECs, NOD/SCID mice were divided randomly into 4 groups (10 mice in each group) that were given either 2×10^6 (low dose) or 4×10^6 (high dose) hAECs, 1.75×10^6 B16-F10 cells or 0.9% NaCl per mouse. Then, the tumor volume and mouse weight were measured every 3 d for 4 months. To investigate whether hAECs affect tumor growth, the NOD/SCID mice were subjected to co-injection of 5×10^4 (low dose), 5×10^5 (medium dose) or 5×10^6 (high dose) hAECs with 3×10^6 HeLa tumor cells or 3×10^6 Raji tumor cells. Then, the tumor volume and mouse weight were measured every 3 d for 7 weeks. The death of mice was also recorded in both assays. The tumor cell lines B16-F10, HeLa and Raji were purchased from Cell Resource Center of Shanghai Institutes for Biological Sciences, Chinese Academy of Sciences.

Reverse transcription-PCR

Total RNA was isolated using an ENZA total RNA Kit (Omega) according to the manufacturer's instructions. cDNAs were generated using a ReverTra Ace qPCR RT kit (Toyobo). Reverse transcription-PCR (RT-PCR) was performed with TaqMix (VWI Science). The primer sequences are listed below: hTERT-F, 5′-AGAGTGTCTGGAGCAAGTTGC-3′ and hTERT-R, 5′-CGTAGTCCATGTTCACAATCG-3′; β-actin-F, 5′-CGCACCACTGGCATTGTCAT-3′ and β-actin-R, 5′-TTCTCCTTGATGTCACGCAC-3′.

Radiation-induced damage model

The NOD/SCID mice were given 2.7 Gy of total body irradiation. Then, 2×10^6 hAECs were transplanted into the mice via iv injection. Body weight and the clinical phenotype, including energy loss, diarrhea, hunching and ruffled hair, were recorded every other day.

Hematoxylin and eosin staining and histological analysis

The mice were sacrificed on d 14 after irradiation, and the lungs and intestines were collected and fixed with 10% neutral-buffered formalin and embedded in paraffin. Then, 5-μm sections were deparaffinized in xylene, rehydrated in ethanol, and stained with hematoxylin and eosin. Histopathological scores were assessed based on the scale system modified from Polchert *et al*[23]. The scores for lungs and intestines are defined as follows: for the lung, 0=normal; 1.0=perivascular cuffing, 1–2 cells in thickness, involving up to 15% of vessels; 2.0=perivascular cuffing, 2–3 cells in thickness, involving up to 15% of vessels and infiltration into the parenchyma proper; 3.0=perivascular cuffing, 4–5 cells in thickness, involving 25%–50% of vessels, and infiltration into the parenchyma proper; 4.0=perivascular cuffing, 6–7 cells in thickness, involving more than 50% of vessels, peribronchiolar cuffing (>6 cells), and infiltration into the parenchyma proper with severe disruption of structure; for the intestine, 0=normal; 1.0=necrotic cells in up to 15% of crypts, minor infiltration of up to 20% of the lamina propria (1–2-cell thickness in intermucosal areas and the submucosa); 2.0=necrotic cells in ≤25% of crypts, infiltration of less than or equal to one-third of the lamina propria (3-cell thickness in intermucosal areas and the submucosa); 3.0=necrotic cells in more than 50% of crypts, infiltration of the lamina propria (5–6-cell thickness in intermucosal areas and the submucosa) with loss of ≤25% of goblet cells; 4.0=necrotic cells in more than 50% of crypts, infiltration of the lamina propria resulting in displacement of more than 50% of the mucosa with loss of 75%–100% of goblet cells.

Statistical analysis

The statistical analysis was performed using GraphPad Prism 5 (GraphPad Software, Inc, San Diego, CA, USA). The

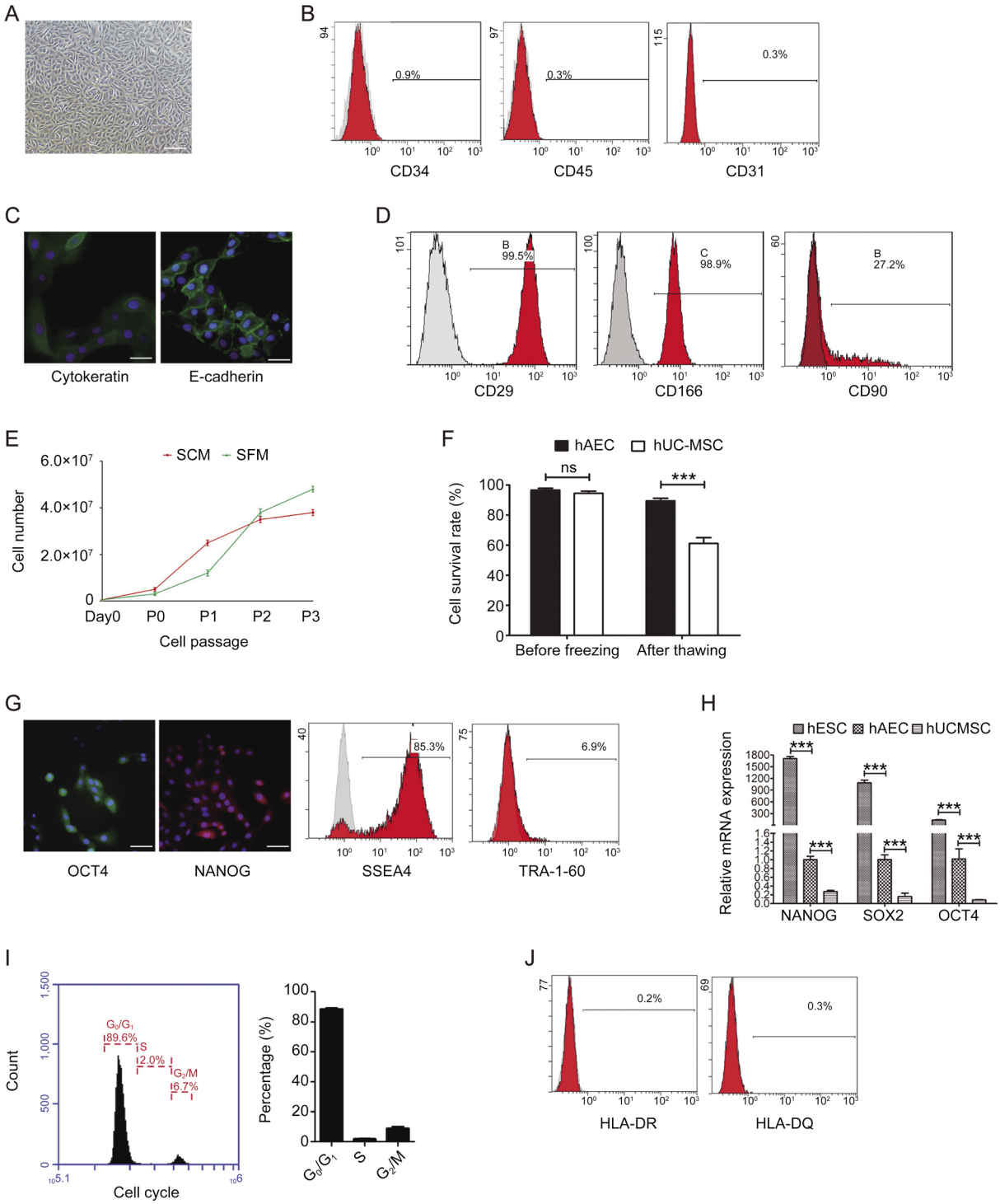

Figure 1. The biological features of hAECs in the serum-free system. (A) Representative light microphotograph of hAECs isolated in the serum-free system; scale bar=200 μm. (B) Flow cytometry detection of the blood cell markers CD45 and CD34 and the endothelial cell marker CD31 in the isolated hAECs. (C) Immunofluorescence microscopy of the epithelium markers pan-cytokeratin (green) and E-cadherin (green) in hAECs. Nuclei were stained with DAPI (blue); scale bar=50 μm. (D) Flow cytometry detection of CD29, CD166 and CD 90 in the isolated hAECs. (E) Growth curves of hAECs in serum and serum-free systems. (F) 5×10^6/mL P1 hAECs or hMSCs were cryopreserved using CELLBANKER serum-free cryopreservation media and thawed after 30 d. The survival rates of hMSCs and hAECs were determined by trypan blue exclusion. (G) Immunofluorescence microscopy and flow cytometry detection of the pluripotent markers OCT4 (green), NANOG (red), SSEA4 and TRA-1-60 in hAECs. Nuclei were stained with DAPI (blue); scale bar=50 μm. (H) Quantitative real-time PCR assessment of the expression of NANOG, SOX2 AND OCT4 in hESCs, hAECs and hMSCs. (I) Representative histogram and statistics of the cell cycle phase distribution of hAECs. (J) Flow cytometry detection of MHC class II markers HLA-DR and HLA-DQ in hAECs.

data are presented as the mean±SEM. The data for these measurements were analyzed using Student's *t*-test or two-way ANOVA. *P* values <0.05 were considered to indicate statistical significance.

Results

The biological features of hAECs in a serum-free system

In the present study, hAECs were isolated and cultured in a serum-free system as described in "Materials and methods". The morphology of hAECs isolated in the serum-free system showed the typical cobblestone-like shape of epithelial cells (Figure 1A). CD34, CD45 and CD31 on the isolated cells were barely detectable (Figure 1B), and the cells stained positive for the epithelial markers cytokeratin and E-cadherin (Figure 1C), suggesting that hAECs isolated by our system were not contaminated with blood cells, endothelial cells or amniotic mesenchymal cells. In addition, regarding epithelial markers, hAECs exhibited full expression of CD29 and CD166 and moderate CD90 expression (Figure 1D, Table 1). In the traditional culture system with serum, the growth of hAECs started to slow down around P2 and obviously appeared inhibited around P3. In contrast, the hAECs in the serum-free system demonstrated a steep growth curve after P1 and a higher total cell yield around P3, although the cell yield was lower before P2 (Figure 1E). These results indicated that the serum-free culture system established in the present study was superior to the traditional serum culture system in delaying hAEC senescence and maintaining their proliferation ability. In addition, serum-free cryopreservation was employed in our system. Most hAECs were detected alive after storage for 30 d followed by thawing, while a significant decrease in the survival rate was observed in human mesenchymal stem cells (hMSCs) (Figure 1F). Importantly, the classical pluripotent markers OCT4, NANOG, SSEA4 and TRA-1-60

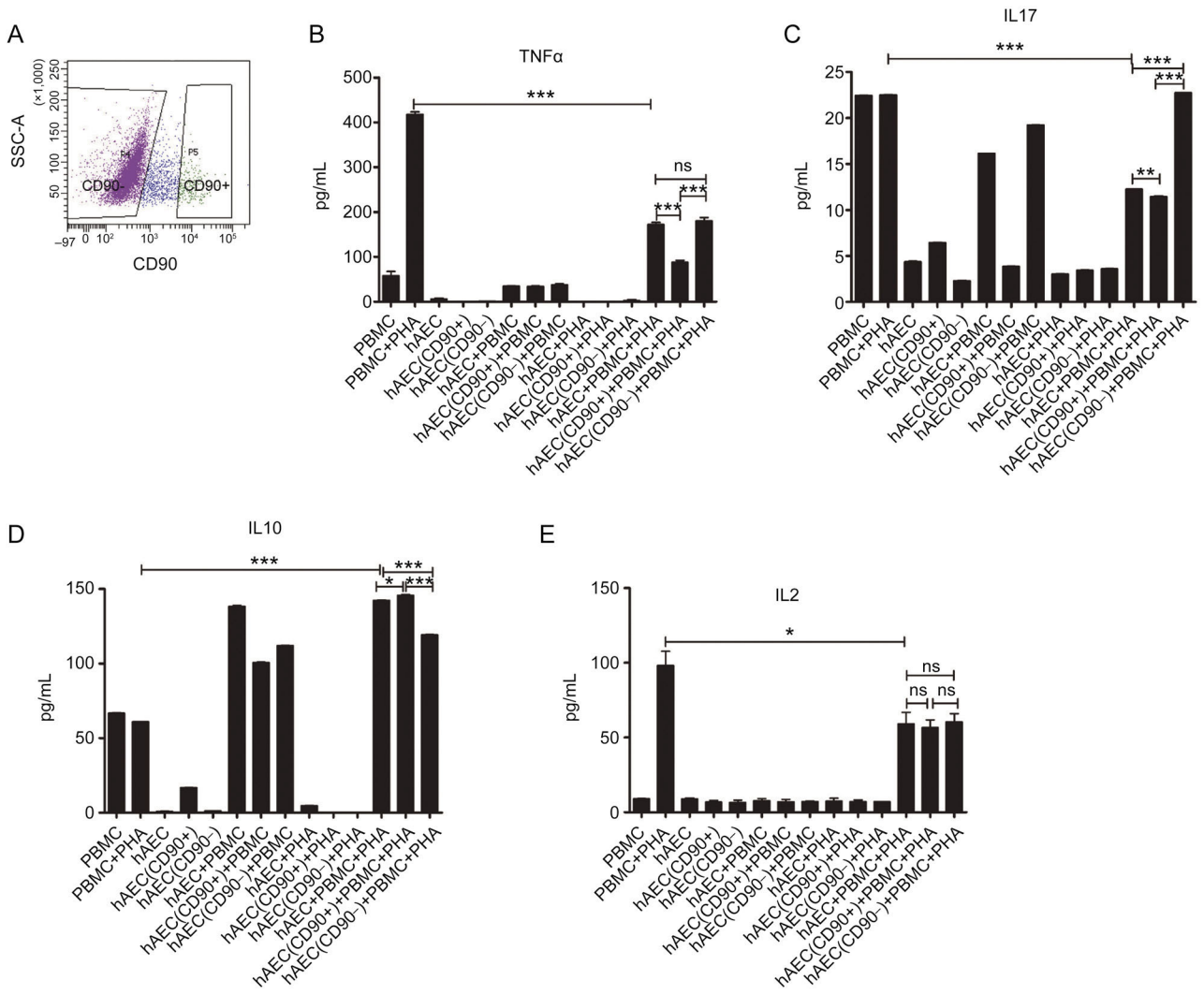

Figure 2. The immunoregulatory properties of hAECs and functional identification of the CD90+ population. Whole hAECs or sorted CD90+ and CD90- hAECs were co-cultured with PHA-activated PBMCs for 3 d. TNFα, IL2, IL17 and IL10 in the culture medium were examined by ELISA. (A) Representative flow cytometry gating for CD90+ and CD90- hAEC sorting. (B–E) ELISA detection of the cytokines TNFα, IL10, IL17 and IL2 in the medium of hAECs.

were sequentially screened and were found to be expressed at different abundance levels in the hAECs cultured in the serum-free system (Figure 1G). Compared with hMSCs, the hAECs expressed even higher levels of the major pluripotent markers (Figure 1H). The cell cycle assay of hAECs revealed typical quiescence, similar to that of most stem cells (Figure 1I). On the other hand, very low levels of HLA-DR and HLA-DQ were detected, indicating weak immunogenicity of the hAECs (Figure 1J). Taken together, the data demonstrated that the hAECs isolated and cultured with the serum-free system were homogeneous and showed robust propagation and maintained pluripotency.

Table 1. The ratio of markers expression in hAECs isolated and cultured in the serum-free system (%).

Pluripotent marker	SSEA-4	79.6±10.3
	TRA-1-60	6.5±2.8
Hematopoietic marker	CD34	0.6±0.2
	CD45	0.4±0.2
Endothelial marker	CD31	0.5±0.3
Mesenchymal stem cell marker	CD29	99.3±0.8
	CD166	99.3±0.5
	CD90	40.4±27.5
MHC-II marker	HLA-DR	0.3±0.1
	HLA-DQ	0.3±0.2

The immunoregulatory properties of hAECs and functional identification of the CD90+ population

To identify the potential immunoregulatory function of hAECs, hAECs were co-cultured with PHA-activated PBMCs. In the presence of hAECs, the pro-inflammatory factors TNFα,

Table 2. Examination of blood routine, blood biochemistry, coagulation index 6 weeks after the last hAECs transplantation in long-term toxicity test.

	Group				
	Control	hAEC (low dose)	hAEC (high dose)	*F* value	*P* value
TP	63.58±5.00	61.39±5.00	62.10±4.00	0.526	0.597
ALB	44.76±7.00	42.15±6.00	42.26±5.00	0.305	0.740
GLOB	18.82±3.00	19.24±1.00	19.84±1.00	1.799	0.186
ALT	29.70±5.00	33.17±7.00	29.44±4.00	0.068	0.935
AST	121.60±2.00	114.48±2.00	119.14±2.00	0.199	0.821
Tbil	2.11±0.00	1.64±0.00	1.83±0.00	0.299	0.744
ALP	63.00±2.00	66.90±3.00	64.40±2.00	0.205	0.816
Bun	6.11±0.00	5.92±0.00	5.55±0.00	0.199	0.821
CREA	41.60±5.00	34.30±4.00	33.30±7.00	1.235	0.307
GLU	6.89±0.00	6.57±0.00	6.49±0.00	0.552	0.583
K	4.24±0.00	4.36±0.00	4.47±0.00	0.332	0.721
Na	142.50±2.00	143.60±1.00	143.50±2.00	0.515	0.604
Cl	99.39±2.00	102.32±1.00	101.27±2.00*	3.865	0.034
TG	0.99±0.00	0.75±0.00	0.83±0.00	0.735	0.489
TCHOL	2.03±0.00	1.76±0.00	1.69±0.00	1.954	0.162
CK	841.00±4.00	719.80±4.00	722.00±2.00	0.538	0.590
WBC	4.57±2.00	3.00±1.00	3.59±0.00	1.875	0.174
RBC	7.53±0.00	7.72±0.00	7.72±0.00	0.307	0.738
HGB	13.49±0.00	13.96±0.00	12.49±3.00	0.243	0.786
HCT	39.64±2.00	41.12±1.00	40.64±0.00	0.290	0.751
PLT	967.60±1.00	922.50±1.00	1021.50±1.00	1.302	0.289
MCV	52.80±3.00	53.37±1.00	52.30±3.00	0.795	0.462
MCH	17.95±0.00	18.11±0.00	17.73±0.00	0.231	0.795
MCHC	34.02±0.00	33.95±0.00	33.58±0.00	0.378	0.689
NEUT%	11.78±4.00	17.99±6.00	11.72±5.00*	3.759	0.037
LYMPH%	84.40±5.00	77.19±6.00	82.75±5.00**	4.988	0.015
MONO%	2.69±0.00	3.36±1.00	3.18±0.00*	3.389	0.049
EO%	1.13±0.00	1.46±0.00	1.34±0.00	1.182	0.323
BASO%	0.00±0.00	0.00±0.00	0.00±0.00	0.581	0.566
RET#	248.44±5.00	227.56±5.00	220.10±3.00	0.052	0.949
APTT	10.50±1.00	12.22±3.00	10.92±2.00	0.448	0.644
Fbg-%	0.19±0.00	0.18±0.00	0.18±0.00	0.064	0.939
Fbg-T	10.35±1.00	10.51±1.00	10.23±1.00	0.202	0.819
PT	9.99±0.00	10.42±0.00	10.24±0.00	0.025	0.975
TT	48.16±6.00	41.77±7.00	45.41±5.00	0.890	0.422

IL17 and IL2 were down regulated, while the anti-inflammatory factor IL10 was upregulated in the culture medium (the 1st, 2nd and 6th columns in Figure 2B-2E). As discussed regarding the basic properties of hAECs, the cell surface marker CD90 was partially expressed in the primary cultured hAECs, suggesting a distinct role of the CD90+ population. To identify whether the CD90+ hAECs possessed a distinct function in immunomodulation, the CD90+ and CD90- hAECs were sorted using flow cytometry and were co-cultured with PBMCs (Figure 2A). The analysis of immunocytokines showed that CD90+ hAECs were the major contributors to TNFα suppression and IL10 promotion compared with CD90- hAECs (Figure 2B, 2D); the decrease in IL17 could also be nearly completely attributed to CD90+ hAECs (Figure 2C). Nevertheless, no significant difference was observed between the CD90+ and CD90- hAECs in the regulation of IL2 (Figure 2E).

Preclinical safety evaluation of hAECs

To assess the preclinical safety of the hAECs isolated and cultured in our system, a systematic safety evaluation was implemented. The toxicity test of hAECs was performed in ICR mice by intravenous injection. The most tolerance dose (MTD) and the no observed adverse effect level (NOAEL) (both were 5.0×10^7 cells/kg) were first identified. Further results of the acute toxicity test showed that both low-dose (the mouse equivalent dose) and high-dose (MTD) hAEC injections induced little toxic response, as evidenced by observations of mouse behavior, mental state, mortality and gross dissection (data not shown) and mouse body weight (Figure 3A, 3B).

Hemolytic and allergy tests were further performed in the recipient animals subjected to hAEC injection. The hemolytic test showed that along with an increased hAEC number, no hemolysis or hemagglutination was identified in a rabbit red cell suspension within 3 h (Figure 3C). On the other hand, similar to the negative control group, no allergic symptoms or associated death was identified in the guinea pigs receiving either a low dose or a high dose of hAECs (Figure 3D, 3E).

To determine the long-term toxicity of hAECs, body weight and viscera weight measurements, hematological examinations and basic histological examinations were performed after 3 hAEC injections in rats for 3 months. The

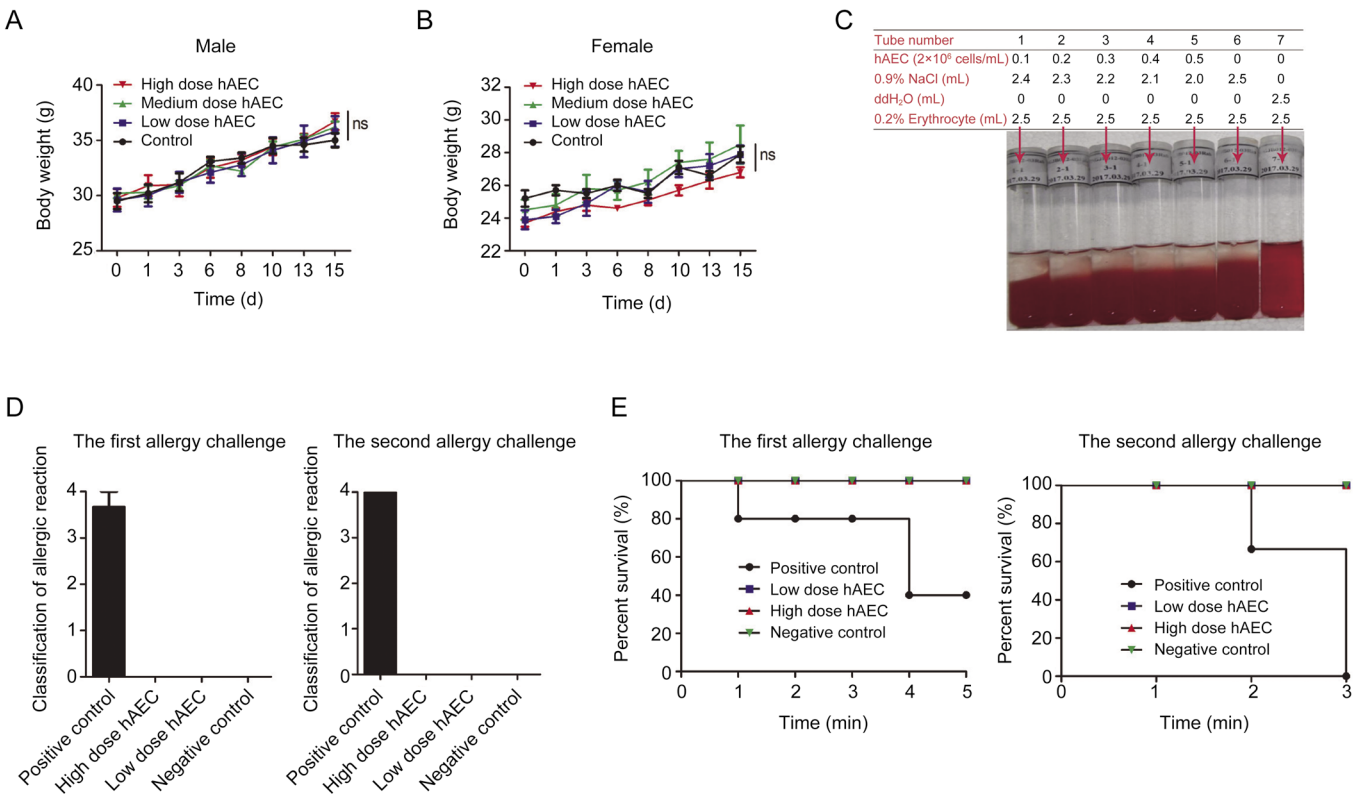

Figure 3. Preclinical safety evaluation of hAECs. The acute toxicity tests of hAECs were performed in ICR mice via single iv injection of hAECs (low dose 2.5×10^7 cells/kg, medium dose 5×10^7 cells/kg or high dose 1×10^8 cells/kg) according to the mouse equivalent dose and the most tolerance dose. Body weight measurements of male and female mice are shown in (A) and (B), respectively; n=10. The hemolysis test of hAECs was performed by co-incubating diluted hAECs with 2% rabbit red blood cell suspension in 0.9% NaCl for 3 h as indicated. A representative picture is shown in (C). The allergy test of hAECs was performed in Hartley guinea pigs via sensitization with 0.5 mL of saline, 5 mg of BSA, 1.0×10^6 hAECs or 2.0×10^6 hAECs followed by two batches of allergy challenges. Quantification of allergic reactions is shown in (D), and the survival curves of each mouse group are shown in (E); n=3.

Table 3. Rats' body weight and viscera weight 6 weeks after the last hAECs transplantation in long-term toxicity test (g).

	Group				
	Control	hAEC (low dose)	hAEC (high dose)	*F* value	*P* value
Body weight	440.78±124.38	397.93±142.54	419.10±158.99	0.226	0.799
Spleen	0.75±0.30	0.73±0.24	0.83±0.30	0.334	0.719
Liver	11.59±3.57	10.62±3.85	11.46±5.06	0.158	0.855
Kidney	2.54±0.72	2.56±0.97	2.73±0.98	0.136	0.873
Heart	1.27±0.34	1.25±0.38	1.28±0.36	0.016	0.984
Brain	1.87±0.15	1.96±0.13	2.00±0.13	2.206	0.130
Lung	1.44±0.31	1.44±0.32	1.57±0.32	0.530	0.595
Adrenal gland	0.06±0.01	0.06±0.01	0.06±0.01	0.016	0.984
Thymus	0.35±0.08	0.32±0.11	0.33±0.07	0.352	0.707
Testis	3.25±0.43	3.43±0.39	3.20±0.42	0.423	0.665
Epididymis	1.25±0.19	1.25±0.21	1.34±0.15	0.352	0.710
Prostate	3.56±0.54	3.83±0.25	4.07±0.41	1.860	0.198
Uterus	0.62±0.11	0.55±0.12	0.61±0.18	0.294	0.750
Ovary	0.13±0.03	0.12±0.02	0.14±0.03	0.440	0.654

results demonstrated that neither the low dose nor the high dose of hAECs affected rat body weight and viscera weight, routine blood parameters, blood biochemistry, or coagulation indexes, but minor changes in neutrophil, lymphocyte and monocyte ratios were observed (Table 2, 3). However, infusion of a high dose of hAECs appeared to recover such changes. In addition, hAEC infusion did not disturb the immune system, as evidenced by little change in the T cell population (Table 4) and no induction of correlated cytokines (data not shown).

Tumorigenicity of hAECs

Tumorigenicity is critical to further affirm the safety of hAECs for clinical application. Therefore, the tumorigenesis of hAECs was determined via hypodermic injection into immunodeficient mice (NOD/SCID); melanoma cells were used as the positive control. Approximately 4 weeks post-injection, the mice receiving melanoma cells died, with melanoma manifesting subcutaneously. In contrast, neither the low-dose nor the high-dose injection of hAECs resulted in any tumor occurrence (Figure 4A–4C). The lack of the telomerase hTERT in hAECs may account for their negative tumorigenicity compared with human ES cells (Figure 4D). Furthermore, compared with the mice receiving tumor cell injection alone, the NOD/SCID mice receiving co-injection of hAECs with HeLa tumor cells demonstrated similar body weights and tumor volumes (Figure 4E, 4F), and the NOD/SCID mice receiving co-injection of hAECs with Raji tumor cells demonstrated a similar survival duration (Figure 4G), indicating that hAECs have little effect on tumor growth.

Therapeutic effect of hAECs on radiation-induced damage in mice

The amniotic membrane-derived cells were considered effective for repairing injuries. To determine the healing ability of hAECs, a radiation-induced damage model was established in mice in the current study. The phenotypes of radiation-induced disease were initially observed in the control mice from the second week after sub-lethal radiation, including body weight loss, energy loss, diarrhea, hunching and ruffled hair. In contrast, hAEC administration evidently alleviated the clinical phenotype of the radiation-induced damage according to body weight measurements and overall ratings (Figure 5A–5C). Consistently, histological examination of the lungs and intestines showed rescued pathological injuries in

Table 4. The ratio of $CD3^+$, $CD4^+$, $CD8^+$ T cell in the whole peripheral blood mononuclear cell 6 weeks after the last hAECs transplantation in long-term toxicity test (%).

	Group				
	Control	hAEC (low dose)	hAEC (high dose)	*F* value	*P* value
$CD3^+$	57.89±7.28	53.22±8.53	51.43±9.13	1.596	0.221
$CD4^+$	48.87±9.50	45.95±7.31	45.98±15.73	0.216	0.807
$CD8^+$	13.43±2.70	15.93±3.17	14.23±5.96	0.925	0.409
$CD4^+/CD8^+$	3.33±0.75	3.01±0.85	3.39±1.17	0.472	0.629

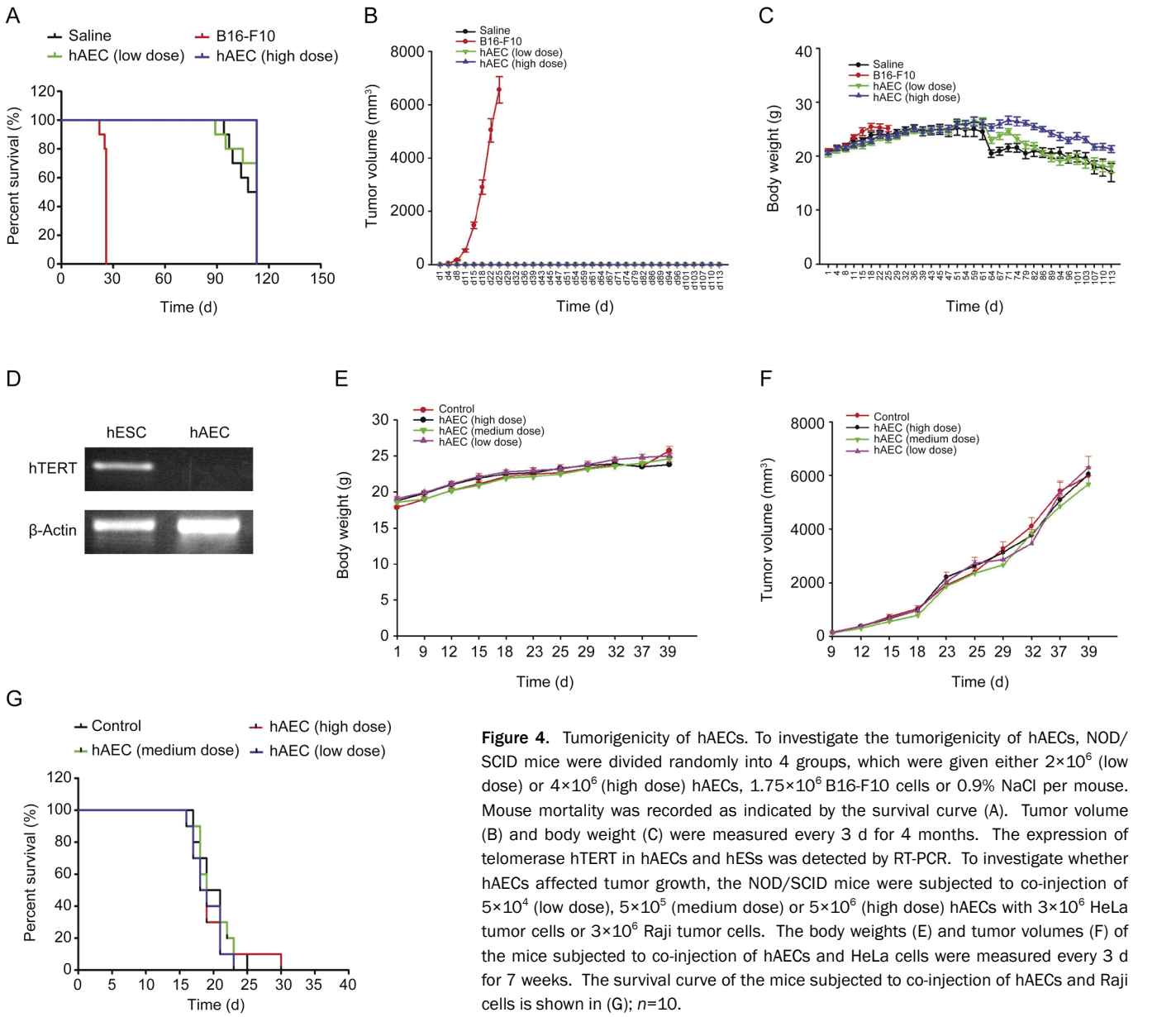

Figure 4. Tumorigenicity of hAECs. To investigate the tumorigenicity of hAECs, NOD/SCID mice were divided randomly into 4 groups, which were given either 2×10^6 (low dose) or 4×10^6 (high dose) hAECs, 1.75×10^6 B16-F10 cells or 0.9% NaCl per mouse. Mouse mortality was recorded as indicated by the survival curve (A). Tumor volume (B) and body weight (C) were measured every 3 d for 4 months. The expression of telomerase hTERT in hAECs and hESs was detected by RT-PCR. To investigate whether hAECs affected tumor growth, the NOD/SCID mice were subjected to co-injection of 5×10^4 (low dose), 5×10^5 (medium dose) or 5×10^6 (high dose) hAECs with 3×10^6 HeLa tumor cells or 3×10^6 Raji tumor cells. The body weights (E) and tumor volumes (F) of the mice subjected to co-injection of hAECs and HeLa cells were measured every 3 d for 7 weeks. The survival curve of the mice subjected to co-injection of hAECs and Raji cells is shown in (G); n=10.

the organs targeted by hAECs (representative images in Figure 5D with quantifications in Figure 5E). In sum, hAEC infusion demonstrated a therapeutic effect on radiation-induced damage *in vivo*.

Discussion

Stem cells have been considered a promising source of seed cells for biological therapeutics and tissue engineering. However, in terms of clinical applications, several safety and ethical criteria are strictly required, which is currently the main limitation for general use of stem cells. In the current study, we focused on hAECs, a unique stem cell population isolated from the epithelium of the human amnion membrane. Targeting clinical application, we established a serum-free integrated system for isolating, culturing and cryopreserving hAECs. By excluding the animal-source constituents, this strategy could prevent serum-derived contamination and toxic effects on hAECs. Indeed, in the serum-free system, hAECs showed better growth ability, maintained regular morphology and cellular quiescence, and exhibited a high revival rate after cryopreservation. In addition, the serum-free system was able to stabilize hAEC quality as evidenced by consistent expression of surface markers and the purity of the hAEC population, indicating reliability and repeatability in the preclinical study. Importantly, low immunogenicity was detected in the hAECs isolated in the new system, indicating the feasibility of allotransplantation without a transplant matching issue. On the other hand, human AE, the origin of hAECs, is obtained from newborn waste and is therefore abundantly available without ethical concerns. Therefore, the hAEC isolation and culture system established in the current study may be an ideal approach for achieving a large-scale supply of seed cells with

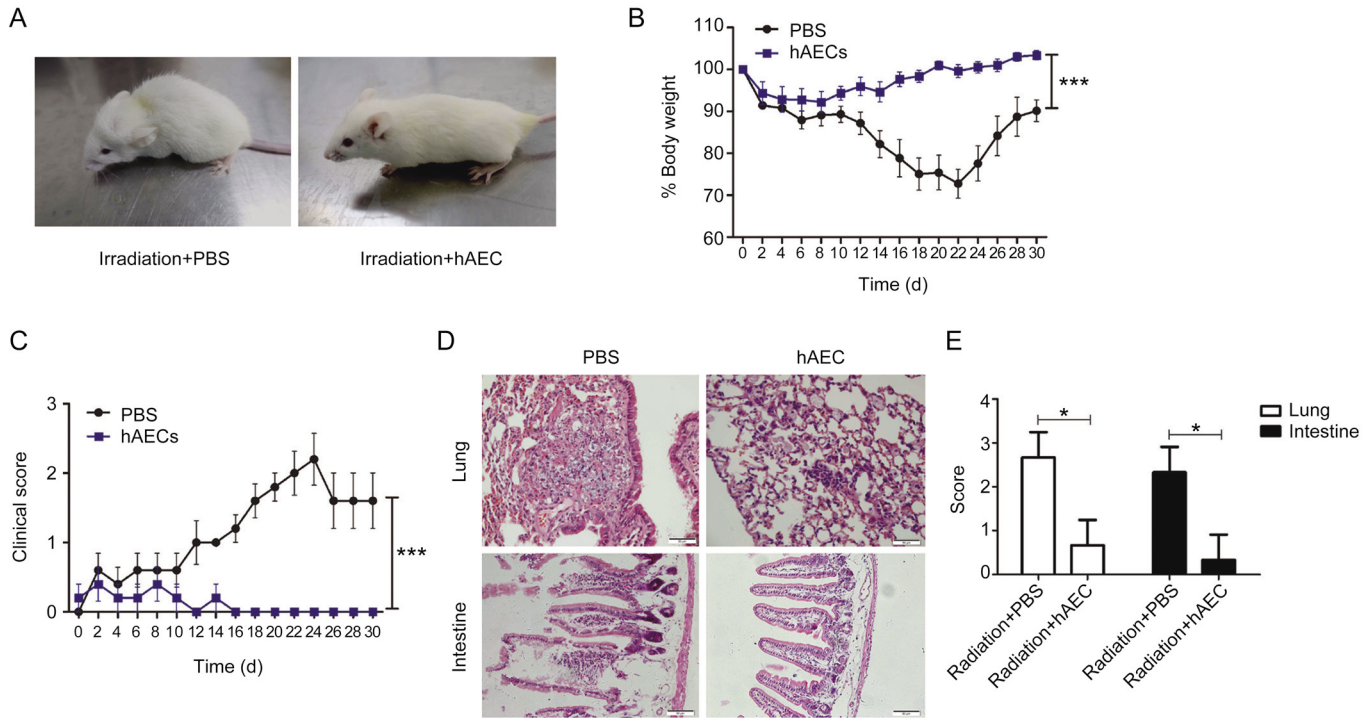

Figure 5. Therapeutic effect of hAECs on radiation-induced damage in mice. The NOD/SCID mice were given 2.7 Gy of total body irradiation (n=5). Then, 2×10^6 hAECs were transplanted into the mice by iv injection. Representative images of the disease phenotype in each mouse group 14 d after hAEC or PBS injection. Body weight measurements in each mouse group. Clinical scores indicating the clinical phenotype, including energy loss, diarrhea, hunching and ruffled hair, in each mouse group. (D, E) Histological examination of the lungs and intestines from each mouse group. Representative H&E staining images (D) and quantifications (E) are shown.

stable and effective qualities for clinical application.

Similar to drugs, the safety of cellular products is considered a priority issue in clinical therapeutics. Therefore, a systemic safety evaluation was conducted on the hAECs following the pattern of drug safety evaluations. Although several basic studies have been conducted, very few safety evaluations have been performed for perinatal stem cells. To our knowledge, the current study is the first to evaluate the preclinical safety of hAECs. In the first part of the evaluation, the MTD and the no observed adverse effect level (NOAEL) were both identified to be 2.5-fold greater than the mouse equivalent dose based on the clinical dose of MSC injection. Further results of the acute toxicity test confirmed that even the MTD had no adverse effect on growth, behavior and general histology. In addition, the negative results of the hemolytic and allergy tests excluded disturbances of the blood system and the immune system induced by hAEC administration, which is supported by the detection of unvaried blood indexes and immune quiescence in the long-term toxicity test. All these results indicate the toxicity and histological safety of hAECs at a potential clinical dose. On the other hand, tumorigenicity is a major concern for stem cell products[24]. Several clinical trials on stem cell therapy have failed due to tumor generation[1, 25, 26], which is caused primarily by reactivation of undifferentiated stem cells. MSCs were reported to promote tumor growth[27]. Therefore, tumor generation and tumor promotion properties of hAECs must be identified. In the current study, assays *in vivo* and *in vitro* revealed that hAECs had no tumorigenicity. Our examination of hAECs in nude mice also supported this conclusion (data not shown). These results ensure the other critical part of safety for the clinical application of hAECs.

Since the beginning of last century, amniotic tissue has been applied to repair burn injuries, ulcers and corneal disease. Recently, many studies have reported the therapeutic potential of hAECs in wound healing[21]. Our previous studies demonstrated the therapeutic effects of hAECs in kidney injury, alveolar defects, premature ovarian failure and ischemia-reperfusion injury after middle cerebral artery occlusion[28-31]. In the present study, we demonstrated the therapeutic effect of hAECs on radiation-induced damage. The results revealed a novel function of hAECs in systemic injury and also confirmed the biological activity of the hAECs cultured in the serum-free system. The first cellular mechanism of hAECs in injury restoration could be attributed to the high degree of plasticity. As shown in the current study, hAECs exhibited higher levels of multipotent markers than MSCs cultured in a similar serum-free system; hAECs may have better plasticity among placenta stem cells based on their derivation from pregastrulation embryonic cells. Indeed, osteogenic, neural and granulosa cell differentiation was observed in our studies mentioned above, while our other study reported that hAECs could differentiate into functional insulin-producing cells[6]. Second, hAECs may

maintain a stable cellular microenvironment to negatively modulate inflammation during injury, which could be due to the specific role of the amniotic membrane in maintaining feto–maternal tolerance. Recent studies have revealed that hAECs can significantly reduce the proliferation of T lymphocytes caused by mixed lymphocyte reaction (MLR) or mitogen PHA[32-34]. Moreover, high levels of programmed death ligand (PD-L) 1 and PD-L2 were detected in IFNγ-treated hAECs, indicating that hAECs inhibited the activation and proliferation of T lymphocytes by initiating their programmed death[32, 35]. On the other hand, hAECs were found to produce a variety of immunoregulatory factors, such as macrophage migration inhibitory factor, TGF-β, IL10, prostaglandin E2, and hepatocyte growth factor, thereby suppressing the functions of inflammatory cells[13, 35-37]. Consistent with this, our previous studies demonstrated the importance of hAEC paracrine activity for injury recovery *in vivo*[28, 38]. Intriguingly, we identified CD90+ hAECs as a unique population with a powerful immunoregulatory capacity, which may be a significant advantage for the clinical application of hAECs. Our further studies will focus on targeted diseases and associated therapeutic strategies based on the current hAEC culture system.

Acknowledgements

This work was supported by the Project of Health Collaborative Innovation of Guangzhou City (Grant No 201704020214), the National Natural Science Foundation of China (Grant No 81770444 and 81600354) and Fundamental Research Funds for the Central Universities of China.

Author contribution

Lu-yang YU, Peng-jie YANG, Wei-xin YUAN and Li-he GUO conceived and designed the experiments; Peng-jie YANG, Wei-xin YUAN, Jia LIU, Jin-ying LI, Chen QIU and Cong QIU performed the experiments; Peng-jie YANG, Wei-xin YUAN, Lu-yang YU, Jia LIU, Bing TAN and Xiao-long ZHU analyzed the data; Peng-jie YANG, Cong QIU and Lu-yang YU wrote and edited the manuscript. All the authors approved the final manuscript.

References

1 Fujikawa T, Oh SH, Pi L, Hatch HM, Shupe T, Petersen BE. Teratoma formation leads to failure of treatment for type I diabetes using embryonic stem cell-derived insulin-producing cells. Am J Pathol 2005; 166: 1781–91.
2 Takahashi K, Tanabe K, Ohnuki M, Narita M, Ichisaka T, Tomoda K, *et al*. Induction of pluripotent stem cells from adult human fibroblasts by defined factors. Cell 2007; 131: 861–72.
3 Zhao T, Zhang ZN, Rong Z, Xu Y. Immunogenicity of induced pluripotent stem cells. Nature 2011; 474: 212–5.
4 Lister R, Pelizzola M, Kida YS, Hawkins RD, Nery JR, Hon G, *et al*. Hotspots of aberrant epigenomic reprogramming in human induced pluripotent stem cells. Nature 2011; 471: 68–73.
5 Miki T. Amnion-derived stem cells: in quest of clinical applications. Stem Cell Res Ther 2011; 2: 25.
6 Hou Y, Huang Q, Liu T, Guo L. Human amnion epithelial cells can be induced to differentiate into functional insulin-producing cells. Acta Biochim Biophys Sin (Shanghai) 2008; 40: 830–9.
7 Miki T, Lehmann T, Cai H, Stolz DB, Strom SC. Stem cell characteristics of amniotic epithelial cells. Stem Cells 2005; 23: 1549–59.
8 Tamagawa T, Ishiwata I, Saito S. Establishment and characterization of a pluripotent stem cell line derived from human amniotic membranes and initiation of germ layers *in vitro*. Human Cell 2004; 17: 125–30.
9 Nichols J, Zevnik B, Anastassiadis K, Niwa H, Klewe-Nebenius D, Chambers I, *et al*. Formation of pluripotent stem cells in the mammalian embryo depends on the POU transcription factor Oct4. Cell 1998; 95: 379–91.
10 Hammer A, Hutter H, Blaschitz A, Mahnert W, Hartmann M, Uchanska-Ziegler B, *et al*. Amnion epithelial cells, in contrast to trophoblast cells, express all classical HLA class I molecules together with HLA-G. Am J ReprodImmunol 1997; 37: 161–71.
11 Akle CA, Adinolfi M, Welsh KI, Leibowitz S, McColl I. Immunogenicity of human amniotic epithelial cells after transplantation into volunteers. Lancet 1981; 2: 1003–5.
12 Ueta M, Kweon MN, Sano Y, Sotozono C, Yamada J, Koizumi N, *et al*. Immunosuppressive properties of human amniotic membrane for mixed lymphocyte reaction. Clin Exp Immunol 2002; 129: 464–70.
13 Liu YH, Chan J, Vaghjiani V, Murthi P, Manuelpillai U, Toh BH. Human amniotic epithelial cells suppress relapse of corticosteroidremitted experimental autoimmune disease. Cytotherapy 2014; 16: 535–44.
14 Hori J, Wang M, Kamiya K, Takahashi H, Sakuragawa N. Immunological characteristics of amniotic epithelium. Cornea 2006; 25: S53–8.
15 Li H, Niederkorn JY, Neelam S, Mayhew E, Word RA, McCulley JP, *et al*. Immunosuppressive factors secreted by human amniotic epithelial cells. Invest Ophthalmol Vis Sci 2005; 46: 900–7.
16 Kim JC, Tseng SC. Transplantation of preserved human amniotic membrane for surface reconstruction in severely damaged rabbit corneas. Cornea 1995; 14: 473–84.
17 Lee SH, Tseng SC. Amniotic membrane transplantation for persistent epithelial defects with ulceration. Am J Ophthalmol 1997; 123: 303–12.
18 Prabhasawat P, Barton K, Burkett G, Tseng SC. Comparison of conjunctival autografts, amniotic membrane grafts, and primary closure for pterygium excision. Ophthalmology 1997; 104: 974–85.
19 Shimazaki J, Shinozaki N, Tsubota K. Transplantation of amniotic membrane and limbal autograft for patients with recurrent pterygium associated with symblepharon. Br J Ophthalmol 1998; 82: 235–40.
20 Trelford JD, Trelford-Sauder M. The amnion in surgery, past and present. Am J Obstet Gynecol 1979; 134: 833–45.
21 Faulk WP, Matthews R, Stevens PJ, Bennett JP, Burgos H, Hsi BL. Human amnion as an adjunct in wound healing. Lancet 1980; 1: 1156–8.
22 Zhao B, Liu JQ, Yang C, Zheng Z, Zhou Q, Guan H, *et al*. Human amniotic epithelial cells attenuate TGF-β1-induced human dermal fibroblast transformation to myofibroblasts via TGF-β1/Smad3 pathway. Cytotherapy 2016; 18: 1012–24.
23 Polchert D, Sobinsky J, Douglas G, Kidd M, Moadsiri A, Reina E, *et al*. IFN-γ activation of mesenchymal stem cells for treatment and prevention of graft versus host disease. Eur J Immunol 2008; 38: 1745–55.
24 Bongso A, Fong CY, Gauthaman K. Taking stem cells to the clinic: Major challenges. J Cell Biochem 2008; 105: 1352–60.
25 Cao F, Lin S, Xie X, Ray P, Patel M, Zhang X, *et al*. *In vivo* visualization of embryonic stem cell survival, proliferation, and migration after cardiac delivery. Circulation 2006; 113: 1005–14.

26 Schuldiner M, Eiges R, Eden A, Yanuka O, Itskovitz-Eldor J, Goldstein RS, *et al*. Induced neuronal differentiation of human embryonic stem cells. Brain Res 2001; 913: 201–5.
27 Lynch ME, Chiou AE, Lee MJ, Marcott SC, Polamraju PV, Lee Y, *et al*. Three-dimensional mechanical loading modulates the osteogenic response of mesenchymal stem cells to tumor-derived soluble signals. Tissue Eng Part A 2016; 22: 1006–15.
28. Liu J, Hua R, Gong Z, Shang B, Huang Y, Guo L, *et al*. Human amniotic epithelial cells inhibit $CD4^+$ T cell activation in acute kidney injury patients by influencing the miR-101-c-Rel-IL-2 pathway. Mol Immunol 2017; 81: 76–84.
29 Jiawen S, Jianjun Z, Jiewen D, Dedong Y, Hongbo Y, Jun S, *et al*. Osteogenic differentiation of human amniotic epithelial cells and its application in alveolar defect restoration. Stem Cells Transl Med 2014; 3: 1504–13.
30 Wang F, Wang L, Yao X, Lai D, Guo L. Human amniotic epithelial cells can differentiate into granulosa cells and restore folliculogenesis in a mouse model of chemotherapy-induced premature ovarian failure. Stem Cell Res Ther 2013; 4: 124.
31 Liu T, Wu J, Huang Q, Hou Y, Jiang Z, Zang S, *et al*. Human amniotic epithelial cells ameliorate behavioral dysfunction and reduce infarct size in the rat middle cerebral artery occlusion model. Shock 2008; 29: 603–11.
32 Insausti CL, Blanquer M, Garcia-Hernandez AM, Castellanos G, Moraleda JM. Amniotic membrane-derived stem cells: immunomodulatory properties and potential clinical application. Stem Cells Cloning 2014; 7: 53–63.
33 Garfias Y, Zaga-Clavellina V, Vadillo-Ortega F, Osorio M, Jimenez-Martinez MC. Amniotic membrane is an immunosuppressor of peripheral blood mononuclear cells. Immunol Invest 2011; 40: 183–96.
34 Banas RA, Trumpower C, Bentlejewski C, Marshall V, Sing G, Zeevi A. Immunogenicity and immunomodulatory effects of amnion-derived multipotent progenitor cells. Hum Immunol 2008; 69: 321–8.
35 Li H, Niederkorn JY, Neelam S, Mayhew E, Word RA, McCulley JP, *et al*. Immunosuppressive factors secreted by human amniotic epithelial cells. Invest Ophthalmol Vis Sci 2005; 46: 900–7.
36 Tahara M, Tasaka K, Masumoto N, Adachi K, Adachi H, Ikebuchi Y, *et al*. Expression of messenger ribonucleic acid for epidermal growth factor (EGF), transforming growth factoralpha (TGF alpha), and EGF receptor in human amnion cells: possible role of TGF alpha in prostaglandin E2 synthesis and cell proliferation. J Clin Endocrinol Metab 1995; 80: 138–46.
37 Koizumi NJ, Inatomi TJ, Sotozono CJ, Fullwood NJ, Quantock AJ, Kinoshita S. Growth factor mRNA and protein in preserved human amniotic membrance. Curr Eye Res 2000; 20: 173–7.
38 Yao X, Guo Y, Wang Q, Xu M, Zhang Q, Li T, *et al*. The paracrine effect of transplanted human amniotic epithelial cells on ovarian function improvement in a mouse model of chemotherapy-induced primary ovarian insufficiency. Stem Cells Int 2016; 2016: 4148923.